

FULL PAPER

Montmorillonite and Beidellite Intercalated with Tetramethylammonium Cations

Pavla Čapková¹, Miroslav Pospíšil¹, Jocelyn Miché-Brendlé², Miroslava Trchová¹, Zdenek Weiss³, and Ronan Le Dred²

¹Faculty of Mathematics and Physics, Charles University Prague, Ke Karlovu 3, 12116 Prague 2, Czech Republic .
E-mail: capkova@quantum.karlov.mff.cuni.cz

²Laboratoire de Matériaux Minéraux (UPRES A CNRS 7016), E.N.S.C. Mu., Université de Haute Alsace, 3 rue A. Werner, F-68093, Mulhouse, France

³Central Analytical Laboratory, Technical University Ostrava, 70833 Ostrava, Czech Republic

Received: 18 Februar 2000/ Accepted: 15 September 2000/ Published: 13 December 2000

Abstract Molecular mechanics simulations, combined with X-ray powder diffraction and infrared spectroscopy, have been used in structure analysis of montmorillonite and beidellite intercalated with tetramethylammonium cations. A complex structure analysis provided us with the detailed structure model, including characterization of the disorder, the total sublimation energy and a charge distribution in the structure of intercalates. The calculated basal spacings (14.36 Å for TMA-montmorillonite and 14.12 Å for TMA-beidellite) are in good agreement with the experimental values (14.31 Å for TMA-montmorillonite and 14.147 Å for TMA-beidellite). Both intercalated structures exhibit positional and orientational disorder in the arrangement of TMA cations, and consequently disorder in layer-stacking. In the present work we analyse the effect of octahedral and tetrahedral substitutions in a 2:1 silicate layer on the arrangement of tetramethylammonium (TMA) cations in the interlayer space of montmorillonite and beidellite. The most significant difference between TMA-montmorillonite and TMA-beidellite is in the charge distribution on the TMA cations and silicate layer. The TMA-beidellite structure is highly polarized, the total charge on one TMA cation is +0.167 e⁻, while the total charge on the TMA cation in montmorillonite is +0.050 e⁻.

Keywords Intercalated clays, Tetramethylammonium-clays, Modeling, Molecular mechanics, Montmorillonite, Beidellite

Introduction

Organoammonium-clays have been studied as sorbents for organic contaminants dissolved in water [1, 2] and photofunctional materials. [3-5] If a clay mineral has metal cations in the cation exchange sites, its surface and interlayer space is hydrophilic and it is not a good sorbent for organic species. However, when the interlayer metal cation is replaced by an organoammonium cation, the surface and interlayer space of the clay become strongly organophilic. [4-6] It has been revealed that the assembly of the intercalated alkylammonium ions acts as a novel support for organizing organic molecules on the surface and in the interlayer space of organoammonium clays. [4-6]

In the present work, we analyze the effect of octahedral and tetrahedral substitutions in the 2:1 silicate layer on the arrangement of tetramethylammonium (TMA) cations in the interlayer space of montmorillonite and beidellite. The structure analysis is based on a combination of molecular mechanics simulation with X-ray powder diffraction and infrared spectroscopy. This complex structure analysis provided us with :

- the detailed structure model, *i.e.* the position and orientation of the TMA cations with respect to the silicate layers, the character of layer-stacking and characterization of the structural disorder.
- the total sublimation energy, including the comparison of host-guest and guest-guest interaction energies.
- the charge distribution on the silicate layer and interlayer cations.

Molecular mechanics simulations have been carried out in the Cerius² modeling environment. Experiment plays a key role in setting up the modeling strategy and in confirmation of the modeling results.

Complementary experiment

Preparation of samples

TMA-montmorillonite was prepared in the Central Analytical Laboratory, Technical University Ostrava. Montmorillonite from Ivancice (Czech republic) was used for the experi-

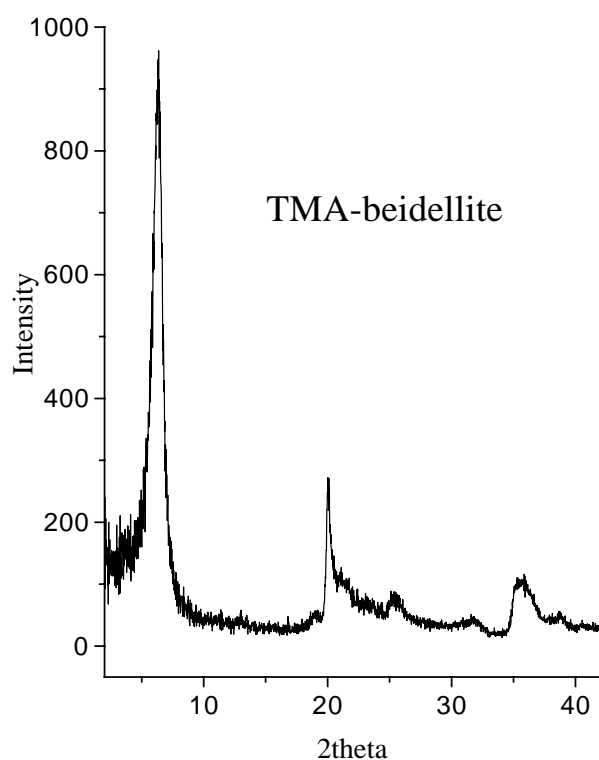


Figure 1 X-ray powder diffraction pattern of TMA-beidellite

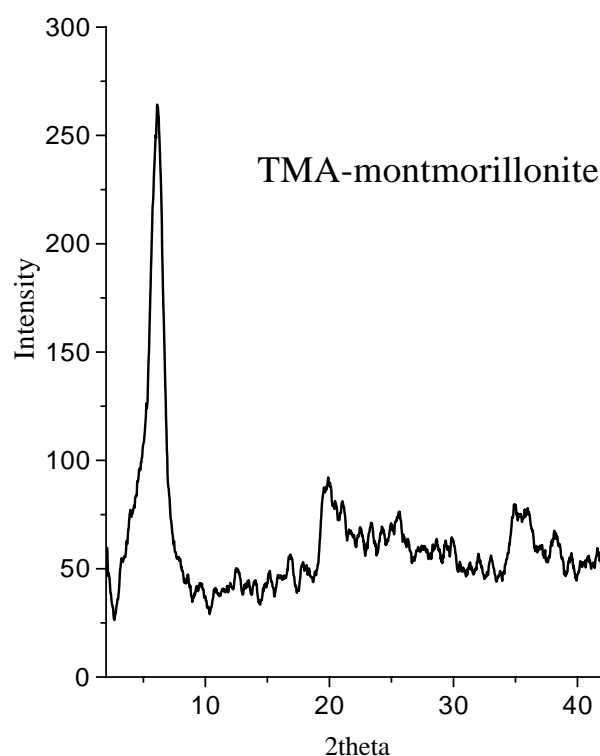


Figure 2 X-ray powder diffraction pattern of TMA-montmorillonite

mental work. The original sample was ground in an agate mortar and the fraction with grain size less than 5 μm was prepared by sedimentation. A saturated sodium form of montmorillonite was prepared from this fraction by shaking with 1 mol·l⁻¹ NaCl solution. Following multiple saturation treatments, the sample was washed with deionized water and air-dried. The following crystallochemical formula was calculated (using the program VZORCE [7]) for fully saturated Na-montmorillonite from the chemical analysis:



Na-montmorillonite was used as the starting material for intercalation by the TMA-cations. Intercalated montmorillonites were prepared by a conventional ion-exchange method using aqueous solutions of tetramethylammonium chloride. The amount of added TMA-chloride was sufficient to give fully saturated TMA-montmorillonite, (i.e. 0.98 mmol TMA-chloride per 1g of montmorillonite). After the ion exchange, the product was washed with deionized water repeatedly until a negative chloride test was obtained. The final product was air-dried at 60°C for 15 hours.

The TMA-beidellite samples were prepared in the Laboratoire de Matériaux, Université de Haute Alsace, the elemental analysis of TMA-beidellite was performed by the service central d'Analyse of the Centre National de la Recherche Scientifique (CNRS). The host clay used to prepare TMA-beidellite was a Na-beidellite synthesized in an acidic fluoride medium under hydrothermal conditions. A hydrogel of the following molar composition: 1 SiO₂; 0.382 Al₂O₃; 0.176 NaF; 0.1 HF; 48 H₂O was prepared. In these conditions, the theoretical layer charge per one unit cell is equal to -1.2 according to the composition: Na_{1.2}(Al₄)(Si_{6.8}Al_{1.2})O₂₀(OH)_{3.04}F_{0.96}. Hydrofluoric acid (HF, Fluka, 5% water) was first added to distilled water, then sodium fluoride (NaF, Prolabo, 98%) was dissolved. After dissolution, the alumina (Al₂O₃, Condea, 75.6%) and silica (SiO₂, Aerosil 130, Degussa, 99.5%) were added. This mixture was matured at room temperature for 2 hours before being heated in a PTFE-lined stainless-steel autoclave at 220 °C under autogenous pressure for 2 days. After crystallization, the product was filtered, washed with distilled water and dried at 60 °C for 12 hours. 1 g of this material was then added to 21.5 ml of a 1M aqueous solution of tetramethylammonium chloride (TMA-Cl, Fluka, >98 %). This mixture was stirred at room temperature for 24 hours. The TMA-exchanged beidellite was separated by centrifugation and thoroughly washed with distilled water, until no chloride ions were detected in the supernatant liquid. The final product was finally dried at 60 °C for 12 hours.

X-ray diffraction measurements (XRD)

The X-ray powder diffraction (XRD) patterns of TMA-beidellite were recorded on a Philips PW1800 automatic powder diffractometer employing CuK α radiation and with automatic divergence slits. The powder diffraction pattern of

TMA-beidellite is shown in Figure 1. Information about the phases present and the d_{001} spacing, which is considered as one of the most characteristic parameters of intercalated clays, was obtained with the APD1700 software.

TMA-beidellite is highly crystalline and virtually pure, as shown by XRD. The spectrum exhibits the characteristic hk bands at 4.44 Å (02,11), 2.55 Å (13,20) and 1.487 Å (06,33). The latter reflexion indicates the dioctahedral nature of the material. The (001) peak is located at 14.147 Å. Thus, the interlayer spacing is 4.547 Å since the basal spacing (d_{001}) equals the thickness of the silicate layer (i.e. 9.60 Å for the beidellite) and the interlayer spacing. Some (00l) reflexions are also present, with a (003) band at 4.68 Å and a (004) band at 3.49 Å. Assuming orthorhombic symmetry, the unit-cell parameters deduced from XRD data are:

$$a = \frac{b}{\sqrt{3}} = 5.15 \text{ \AA}, b = 6 \times d_{060} = 8.92 \text{ \AA}, c = 14.147 \text{ \AA}.$$

The X-ray powder diffractograms of TMA-montmorillonite were measured on an INEL powder diffractometer with a PSD 120 position sensitive detector, under the following conditions: reflection mode, rotating sample holder (capillary), CuK α radiation, mixture of silicon and Ag-behenate was used as a calibration standard for PSD. The powder diffraction pattern of TMA-montmorillonite is shown in Figure 2. The profile fitting was done by the DIFPATAN program. [8] The estimated basal spacing was $d = 14.31 \text{ \AA}$. The powder diffraction pattern of TMA-montmorillonite exhibits the same characteristic features as TMA-beidellite with the hk-bands indicating the turbostratic layer stacking. The fact that the positions of hk-bands are the same in powder pattern of the host structures and intercalates, and consequently the a and b parameters of silicate layer remain the same, confirms the rigidity of the silicate layers.

Infrared spectroscopy

The structural and optical properties of the TMA-montmorillonite were checked using Fourier transform infrared (FTIR) spectroscopy. Infrared measurements were performed on a Nicolet IMPACT 400 FTIR spectrometer in an H₂O-purged environment. All spectra in the range 400 – 4000 cm⁻¹ with 2 cm⁻¹ spectral resolution were obtained from compressed KBr pellets in which the samples were evenly dispersed. Two hundred scans were used to record each FTIR spectrum. The spectra were corrected for the H₂O and CO₂ content in the optical path.

Figure 3 shows the comparison of IR spectra of the host structure Na-montmorillonite and intercalate TMA-montmorillonite and TMA-chloride. The structure of TMA-chloride exhibits the characteristic absorption bands of TMA-cations corresponding to: (1) C-H stretching mode of methyl group (asymmetrical at ~ 3005 cm⁻¹ and symmetrical at ~ 2925 cm⁻¹); (2) C-H bending mode of the methyl group (asymmetrical at ~ 1489 cm⁻¹ and symmetrical at ~ 1403 cm⁻¹);

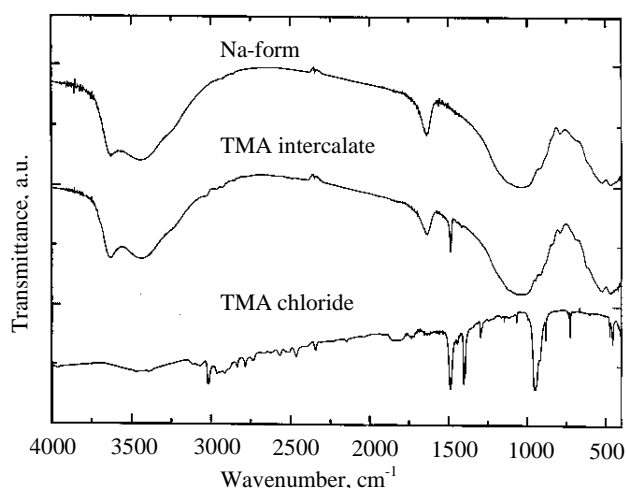


Figure 3 Comparison of IR spectra of the host structure Na-montmorillonite, guest compound TMA-chloride and the intercalate TMA-montmorillonite

and (3) N-C asymmetrical skeletal (tetrahedral) stretching at $\sim 950\text{ cm}^{-1}$ overlapped with methyl rocking vibration at $\sim 946\text{ cm}^{-1}$. (Peak assignment according to Silverstein et al. 1991 [9]). As one can see in Figure 3, the IR spectrum of intercalate preserves all the characteristic absorption bands of the host structure – Na-montmorillonite. The IR spectrum of TMA intercalate also exhibits the strong peak corresponding to asymmetrical C-H bending of methyl group at $\sim 1489\text{ cm}^{-1}$. The other TMA absorption bands such as the symmetrical and asymmetrical C-H stretching, the symmetrical C-H bending and the skeletal N-C stretching are suppressed in the IR spectrum of the intercalate; *i.e.* the corresponding vibration modes exhibit only broad shoulders on the IR spectrum of the intercalate. This broadening of absorption bands is caused by the crystal field surrounding the TMA cations in the interlayer space of montmorillonite. The positions and orientations of TMA cations in the interlayer are not regular, as in vermiculite. [10, 11] Consequently, due to this disorder, the methyl groups may be anchored differently to the silicate layers, and they can also reside in the central part of the interlayer space (see figures 4a and 5a). These irregularities in position and orientations of methyl groups result in wider range of vibrational frequencies; *i.e.* in broadening and weakening of the corresponding absorption bands in the IR spectrum of intercalate.

Strategy of modeling

The host-guest interactions in phyllosilicates intercalated with organic and inorganic cations are of a non-bonded nature. This generally accepted opinion is based on the character of the intercalation reaction (an ion exchange) and confirmed by the present vibrational spectroscopic measurements. This

is also the basic assumption in the modeling strategy. Following the results of XRD diffraction and IR spectroscopy, the rigidity of silicate layers have been found to be a reasonable approximation for the modeling strategy. As to the guest species, we have chosen two ways:

- **Rigid silicate layers and rigid TMA cations.** Assuming rigid layers and rigid guest cations during energy minimization, we can use the *Crystal Packer* module in the *Cerius²* modeling environment, which leads to significant reduction of CPU time for the calculations.
- **Rigid silicate layers, variable bonding geometry of TMA cations.** In this case, the energy minimization has been performed using the *Minimizer* module in *Cerius²*.

Crystal Packer is a computational module that estimates the total sublimation energy and packing of molecular crystals. Energy calculations in *Crystal Packer* only take into account the non-bond terms, *i.e.* van der Waals interactions (VDW), Coulomb interactions (COUL), hydrogen bonding (H-B), internal rotations and hydrostatic pressure. The asymmetric unit of the crystal structure is divided into fragment-based rigid units. Non-bond (VDW, COUL, H-B) energies are calculated between the rigid units. During the energy minimization, the rigid units can be translated and rotated and the unit cell parameters varied.

The Ewald summation method is used to calculate the Coulomb energy in a crystal structure. [12] The Ewald sum constant was 0.5 \AA^{-1} . The minimum charge taken into the Ewald sum was 0.00001e. All atom pairs with separations less than 10 \AA were included in the real-space part and all reciprocal-lattice vectors with lengths less than 0.5 \AA^{-1} were included in the reciprocal part of the Ewald summation. Charges in the crystal are calculated in *Cerius²* using the QEq-method (Charge equilibrium approach. [13] For VDW we used the well-known Lennard-Jones functional form, with the arithmetical radius combination rule. A non-bond cut-off distance for the VDW interactions was 7.0 \AA .

There are three force fields available in *Crystal Packer* for VDW parameters: Tripos, [14] Universal [15] and Dreiding. [16] In our previous paper [10] we tested the convenience of these force fields for modeling of clays intercalated with organoammonium cations. The results of modeling were compared with the structure parameters obtained from single crystal diffraction data for vermiculite intercalated with tetramethylammonium and aniline. Best agreement between calculated and experimental results was obtained with the Tripos force field. (For more details see [10]). An additional test using *ab initio* calculations (*Gaussian*) confirmed Tripos as the most convenient force field for the layered silicates intercalated with organic molecules. [10]

Initial models

Initial models for montmorillonite were built using structure data published by Tsipursky and Drits (1984), [17] space group *C2/m*. The unit cell parameters according to Méring (1967) [18] have been used to define the planar unit cell dimensions: $a = 5.208\text{ \AA}$ and $b = 9.020\text{ \AA}$. The silicate layers were

Table 1 Average values of the calculated basal spacing d , the total sublimation energy E_S and the corresponding fluctuation range of d - and E_S -values for TMA-montmorillonite (TMA-MMT) and TMA-beidellite (TMA-BEID). All the calculated energy values are related to one supercell $2a \times 2b \times 1c$

	d (Å)	d -range (Å)	E_S (kcal·mol ⁻¹)	E_S -range (kcal·mol ⁻¹)
TMA-MMT	14.36	14.02 – 14.52	1181.6	1156.8 – 1202.6
TMA-BEID	14.12	13.89 – 14.29	1129.7	1122.3 – 1137.4

removed to a distance of 14.5 Å, allowing the placement of the TMA-cations into the interlayer space. Assuming a composition of the montmorillonite layer of $(Al_3Mg_1)Si_8O_{20}(OH)_4$ the supercell $2a \times 2b \times 1c$ was built, with a total layer charge (-4) and consequently with four TMA-cations in the interlayer space. This means that 5 rigid units are assigned to this supercell: 4 TMA-cations and montmorillonite layer.

The initial model for beidellite was built using the same size of supercell $2a \times 2b \times 1c$, where the cell parameters $a = 5.15$ Å and $b = 8.92$ Å were determined by a profile analysis of the XRD powder pattern. Assuming the crystallochemical formula of the beidellite layer to be $(Al_4)(Si_7Al_1)O_{20}(OH)_4$, which is a reasonable approximation of the real sample composition (see Preparation of samples), 5 rigid units were assigned to this model: 4 TMA-cations and beidellite layer.

Results

Structure of TMA-montmorillonite and TMA-beidellite

The arrangement of TMA cations in the interlayer space of montmorillonite is illustrated in Figures 4 and 5 for two different minimized models with nearly the same total sublimation energy. While for the model TMA-MMT-I in Figure 4a,b the total sublimation energy per supercell was 1202.6 kcal·mol⁻¹, basal spacing $d = 14.334$ Å, for the model TMA-MMT-II the total sublimation energy per supercell was 1201.6 kcal·mol⁻¹, basal spacing $d = 14.478$ Å. As one can see in both figures, the TMA cations are not regularly ordered as to their orientation and position with respect to the silicate layer. The same character of disorder in the arrangement of the TMA-cations has been observed in the case of beidellite. A series of initial models of TMA-montmorillonite and TMA-beidellite was built for the energy minimization with different starting positions and orientations of TMA cations in the interlayer space and with different arrangements of the tetrahedral and octahedral substitutions in the silicate layer. As a result of minimization, we have obtained a series of structure models with different arrangements (i.e. positions and orientation of TMA cations) and with different basal spacing, but with nearly the same total sublimation energy. This result showed that the system does not exhibit a deep global minimum and that the energy minimum has the shape of a plateau with a series of shallow minima having the same (or

nearly the same) energy. This is a clear indication of structural disorder. Comparison and analysis of all the minimized models can reveal the character of the disorder. In the case of TMA-montmorillonite and TMA-beidellite, the structures exhibit disorder in the positions and orientations of TMA cations with respect to the silicate layer and consequently disorder in layer-stacking. This result is in agreement with the observed diffraction pattern for both structures.

The average value of the basal spacing calculated from the series of minimized models is $d = 14.36$ Å for TMA-montmorillonite and $d = 14.12$ Å for TMA-beidellite. The experimental values are 14.31 for TMA-montmorillonite and 14.147 for TMA-beidellite. Table 1 contains the comparison of results for TMA-montmorillonite and TMA-beidellite, where E_S is the average value of the total sublimation energy, and d -range and E_S -range are the fluctuation ranges of d - and E_S values for the series of calculated models.

No correlation has been observed between the d -value and total sublimation energy E_S within an estimated fluctuation range. For example: two minimized models of TMA-montmorillonite with the same E_S value 1185 kcal·mol⁻¹ and with the same arrangement of the octahedral Al→Mg substitutions have d -values of 14.33 Å and 14.48 Å. The rearrangement of the octahedral Al→Mg substitutions may have a slight effect on the total sublimation energy, which may change within the given range (see table 1), but no correlation has been found between the arrangement of octahedral substitutions and the d -value. The same conclusion as to the relationship between the d -value, total sublimation energy and arrangement of tetrahedral Si→Al substitutions can be derived for TMA-beidellite.

The average total sublimation energy for TMA-montmorillonite $E_S = 1181.6$ kcal·mol⁻¹ consists of a Van der Waals contribution $E_{VDW} = 51.78$ kcal·mol⁻¹ and as electrostatic contribution $E_{COUL} = 1129.8$ kcal·mol⁻¹. In the case of TMA-beidellite the $E_S = 1129.7$ consists of: $E_{VDW} = 55.0$ kcal·mol⁻¹ and $E_{COUL} = 1074.7$ kcal·mol⁻¹. In both cases, the electrostatic interactions are predominant. It seems to be a paradox that the lower total sublimation energy and lower Coulombic energy in the case of beidellite leads to a lower value of the basal spacing. The value of the basal spacing is a result of competition between the host-guest and guest-guest interactions. The mutual relation between the host-guest and guest-guest interaction is different in TMA-MMT and TMA-BEID, thanks to the different charge distribution in the two structures. The higher total charge of TMA-cations in beidellite leads to stronger repulsion between them and consequently

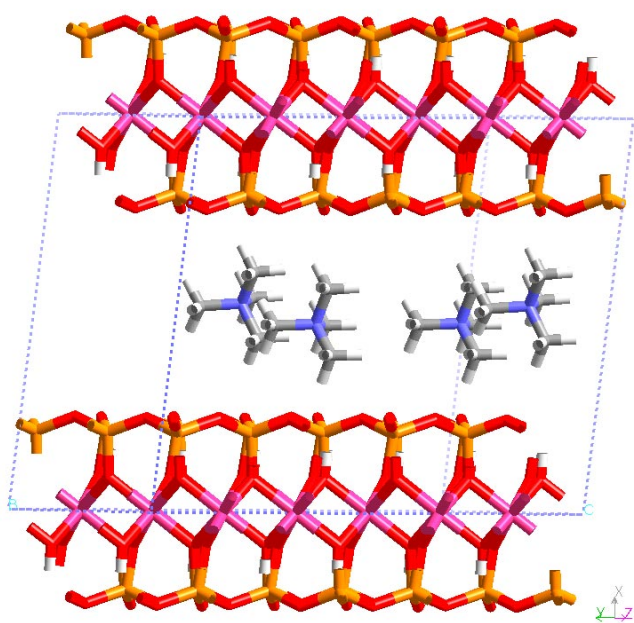


Figure 4a Model TMA-MMT-I: Arrangement of TMA-cations in the interlayer space of TMA-montmorillonite (side view)

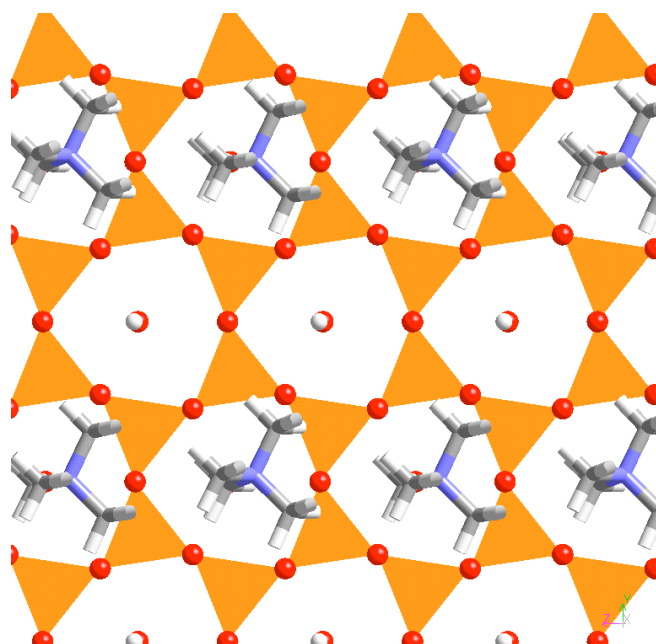


Figure 4b Model TMA-MMT-I: upper view perpendicular to silicate layer

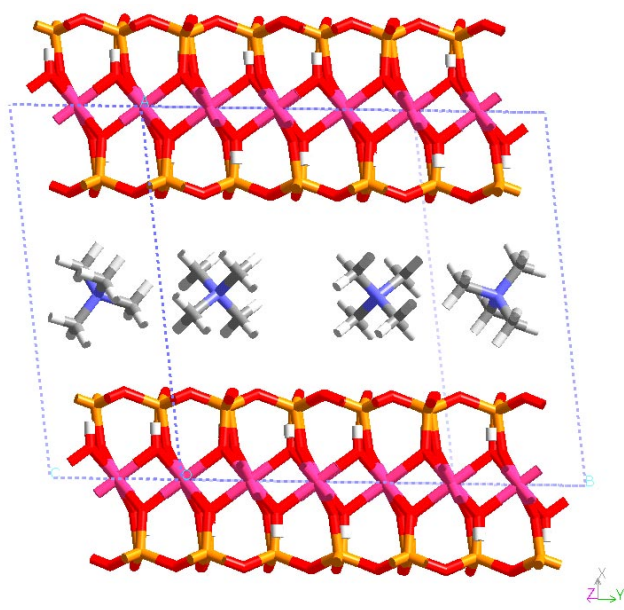


Figure 5a Model TMA-MMT-II: Arrangement of TMA-cations in the interlayer space of TMA-montmorillonite (side view)

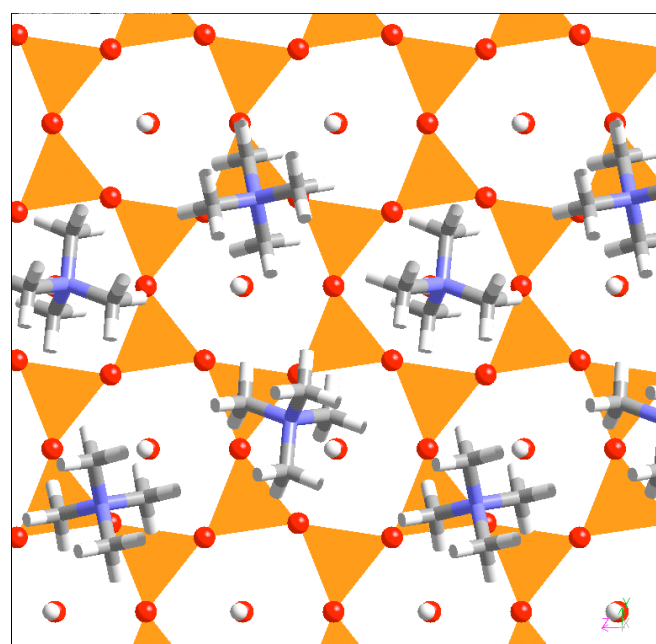


Figure 5b Model TMA-MMT-II: upper view perpendicular to silicate layer

to a decrease of the total sublimation energy of TMA-beidellite.

Energy minimization with rigid silicate layers and variable bonding geometry of TMA cations was performed using the *Universal force field*, as the only convenient force field in the *Minimizer* module. This strategy led to the same re-

sults as to the disorder of TMA cations in the interlayer space. The results of energy minimization also showed that comparing the models with fixed and variable TMA bonding geometry, there are negligible changes in N-C bonding distances $\sim 0.001 - 0.002 \text{ \AA}$. The changes in C-H bonding distances are $\sim 0.003 - 0.01 \text{ \AA}$, the changes in tetrahedral angles C-N-C

Table 2 Total charges per one supercell calculated on the silicate layer for the individual sheets of atomic planes in electron units. Q -silicate layer is the total charge on the silicate layer per one $2a \times 2b \times 1c$ supercell and Q -TMA is the total charge on one TMA cation

Charges (el. units)	TMA – MMT	TMA - BEID
Charge fluctuation on the surface oxygen atoms	-0.63 – (-0.66)	-0.61 – (-0.66)
Q-oxygen (surface)	-15.335	-15.382
Q-Si/Al (tetr. cations)	+20.648	+20.216
Q-H	+1.758	+1.775
Q-oxygen (apical+O _H)	-16.052	-16.602
Q-Al/Mg (oct. Cation)	+17.77	+19.316
Q-silicate layer (total)	-0.200	-0.668
Q-TMA cation	+0.050	+0.167

are ~ 0.8 – 1.0° . The most pronounced changes have been observed for the H-C-H angles in the methyl groups, which fluctuate for variable TMA geometry between 104.7 – 109.9° . These results also explain the differences in IR spectra of TMA-intercalate and TMA guest compound.

Analysis of the charge distribution in TMA-montmorillonite and TMA-beidellite

Table 2 summarizes the results of charge analyses for TMA-montmorillonite and TMA beidellite. The total charge Q in one supercell was calculated for the individual atomic sheets in the silicate layer. As one can see from the table 2, there are differences between TMA-MMT and TMA-BEID in the layer charge of the surface oxygen sheet, and in the fluctuation range in the surface oxygen charges. While in TMA-MMT the charge on the surface oxygen atoms varies within the range -0.63 – $(-0.66) e^-$, for TMA-BEID the corresponding fluctuation range is -0.61 – $(-0.66) e^-$.

Thanks to charge transfer between the TMA cations and silicate layer, the most significant differences between the charge distributions can be observed for the central part of the silicate layer, i.e. for the octahedral cations and adjacent oxygen sheet. The total charge of the silicate layer per 2×2 supercell for TMA-MMT (Q-silicate layer = -0.200) and for TMA-BEID (Q-silicate layer = -0.668), consequently the total charge per one TMA cation is $+0.050$ in TMA-MMT and $+0.167$ in TMA-BEID. This means, that the charge polarization between the host layer and guest cations is much higher in TMA-beidellite than in TMA-montmorillonite. This higher TMA and layer charge leads to the stronger host-guest interaction in beidellite, and consequently to the lower basal spacing. On the other hand, the higher TMA charge in beidellite leads to a higher mutual repulsion between the guest cations in the interlayer, which results in a lower total sublimation energy in case of TMA-beidellite.

Discussion and conclusions

The present results show that the intercalation behavior of montmorillonite and beidellite is very similar, in the disorder in arrangement of TMA-cations and in the turbostratic stacking of layers. The main difference between TMA-montmorillonite and TMA-beidellite is in host-guest charge distribution, which leads to a different mutual relation between the host-guest and guest-guest interaction energies in the two intercalates. This difference results in a slightly lower average basal spacing and total sublimation energy in case of beidellite.

Results of modeling for TMA-montmorillonite and TMA-beidellite are in good agreement with the XRD measurement for the basal spacing and the character of the disorder (the turbostratic layer stacking observed in diffraction pattern was confirmed by modeling. The fluctuation of d -values, which is higher in the case of TMA montmorillonite (14.02 \AA – 14.52 \AA) than for TMA-beidellite (13.89 \AA – 14.29 \AA) was confirmed by the comparison of 001 line width in the two diffractograms. The full width at half-maximum FWHM of 001 reflection was estimated $\sim 1^\circ$ in 2θ for TMA-beidellite and 1.2° in 2θ for TMA-montmorillonite.

A similar structure of TMA-vermiculite has been studied by Vahedi-Faridi and Guggenheim [11] using X-ray single crystal diffraction. In contrast to our results, the TMA-vermiculite exhibits a regular arrangement of TMA cations and 3D-ordered intercalated structure. This is a result of higher layer charge in the case of vermiculite, which requires a higher concentration of guests in the interlayer and consequently stronger host-guest and guest-guest interactions. A more detailed comparison of modeling and experiment in structure analysis of TMA-vermiculite is given in our previous paper. [10]

The present structure analysis also showed that the molecular mechanics simulation combined with XRD and IR measurement can provide us with a detailed structure model, including characterization of the disorder and with the analysis of charge distribution and the total sublimation energy.

Acknowledgement: This work was supported by the Grant Agency of Czech Republic - GACR, grant no.: 205/99/0185, Grant Agency of Charles University – GAUK, grant no: 37/97/B and by Ministry of Education of Czech Republic, project VZ 113 000.

References

1. Lee, J. F.; Mortland, M. M.; Chiou, C. T.; Kile, D. E.; Boyd, S. A. *Clays Clay Miner.* **1990**, *38*, 113-120.
2. Jaynes, W. F.; Boyd, S. A. *Soil Sci. Soc. Am. J.*, **1991**, *55*, 43-48.
3. Seki, T.; Ichimura, K. *Macromolecules*, **1990**, *23*, 31-35.
4. Ogawa, M.; Kuroda, K. *Chem. Rev.* **1995**, *95*, 399-438.
5. Ogawa, M.; Kimura, H.; Kuroda, K.; Kato, C. *Clay Science*, **1996**, *10*, 57-65.

6. Ogawa, M.; Wada, T.; Kuroda, K. *Langmuir*, **1995**, *11*, 4598-4600.
7. Rieder, M. Computer program *Vestník*, **1977**, *52*, 333-336.
8. Kuřel, R. Jr.; DIFPATAN, Computer program for X-ray powder diffraction profile analysis, Faculty of Mathematics and Physics, Charles University Prague, Czech Republic, **1991**.
9. Silverstein, R. M.; Bassler, G. C.; Morrill, T. C. *Spectrometric identification of organic compounds*, 5th ed., John Wiley & Sons, Inc., New York, 1991.
10. Čapková, P.; Burda, J. V.; Weiss, Z.; Schenk, H. *J.Mol.Model.* **1999**, *5*, 8 – 16.
11. Vahedi-Faridi, A.; Guggenheim, S. *Clays Clay Miner.* **1997**, *45*, 859 – 866.
12. Karasawa, N.; Goddard, W. A., III. *J. Phys. Chem.* **1989**, *93*, 7320 – 7327.
13. Rappe, A. K.; Goddard, W. A., III. *J. Phys. Chem.* **1991**, *95*, 3358 – 3363.
14. Clark, M.; Cramer, R. D., III; Van Opdenbosh, N. *J. Comp. Chem.* **1989**, *10*, 982 - 1012.
15. Rappe, A. K.; Casewit, C. J.; Colwell, K. S.; Goddard, W. A., III; Skiff, W. M. *J. Amer. Chem. Soc.* **1992**, *114*, 10024 – 10035.
16. Mayo, L. S.; Olafson, B. D.; Goddard, W. A., III. *J. Phys. Chem.* **1990**, *94*, 8897- 8909.
18. Tshipursky, S. J.; Drits, V. A. *Clay Miner.* **1984**, *19*, 177 – 193.
18. Méring, J.; Oberlin, A. *Clays Clay Miner.* **1967**, *27*, 3 – 18.